Velocity and pressure measurements in guide vane clearance gap of a low specific speed Francis turbine

B S Thapa[1], O G Dahlhaug[1], B Thapa[2]

[1]Dept. Energy & Process Engineering, Norwegian University of Science and Technology, NTNU, Trondheim, 7491, Norway
[2]Dept. Mechanical Engineering, Kathmandu University, P.O. Box 6250, Dhulikhel, Nepal

Email: biraj.s.thapa@ntnu.no

Abstract. In Francis turbine, a small clearance gap between the guide vanes and the cover plates is usually required to pivot guide vanes as a part of governing system. Deflection of cover plates and erosion of mating surfaces causes this gap to increase from its design value. The clearance gap induces the secondary flow in the distributor system. This effects the main flow at the runner inlet, which causes losses in efficiency and instability. A guide vane cascade of a low specific speed Francis turbine has been developed for experimental investigations. The test setup is able to produce similar velocity distributions at the runner inlet as that of a reference prototype turbine. The setup is designed for particle image velocimetry (PIV) measurements from the position of stay vane outlet to the position of runner inlet. In this study, velocity and pressure measurements are conducted with 2 mm clearance gap on one side of guide vane. Leakage flow is observed and measured together with pressure measurements. It is concluded that the leakage flow behaves as a jet and mixes with the main flow in cross-wise direction and forms a vortex filament. This causes non-uniform inlet flow conditions at runner blades.

1. Introduction

Francis turbine is a reaction machine, which converts both pressure energy and kinetic energy in fluid to the mechanical energy at the runner. Conversion of a part of this pressure energy into the kinetic energy is done by guide vanes (GV). The energy conversion incurs high velocities and high acceleration, which causes unsteady flow phenomenon as wakes and pressure pulsations. GV also direct the fluid into the runner blades at an angle appropriate to the design. GV is pivoted and can be controlled by using a suitable governing mechanism to regulate the flow while the load in the generator changes. Often NACA airfoils are chosen for shaping of GV. However, optimization of profiles are often done to maximize the overall turbine efficiency and minimize the operational constraints. Design of GV is usually combined together with the design of stay vanes, and both components as a single unit in a reaction turbine is often called as the distributor system.

GV imparts a tangential velocity and hence an angular momentum or spin to the water before it enters to the runner. This makes GV positioned such that at two points, along the same chord length, are located at different radii. Thus despite of uniform airfoil structure GV will have a pressure side and a suction side. A dry clearance between GV and cover plates usually exists from the design to allow GV to be positioned, so as to maintain the desire flow. Typical design value of such dry clearance ranges from 0.1 mm to 0.3 mm, depending upon the designs and operating conditions. Due to deflection of cover

plates under high pressure the clearance further increase. Leakage flow starts from the clearance gap due to inherit pressure difference between adjacent GV surfaces. Flow with spin, together with leakage flow from the GV clearance gap, and wakes and vortices from the GV trailing edge make the flow non-uniform. This non-uniform flow field further interacts with rotating runner as each blade passes GV, which is also called as rotor-stator interaction. Thus the flow conditions at runner inlet in a reaction machines becomes very complex.

Chen [1] has done a study on flow field in distributor of a high head Francis turbine and concluded that the exit flow from the guide vane cascade is neither uniform in circumferential direction, nor in span wise direction. Eide [2] has investigated the effects of head cover deflection on flow field and found that clearance gap induces leakage flow and vortices from trailing edge of GV. Brekke [3] has investigated the influence of the guide vane clearance gap on turbine efficiency. He measured a decrease of 0.5 % efficiency at BEP in a prototype with 0.5 mm clearance gap compared to the original runner with 0.3 mm clearance gap. These studies suggest that secondary flow occurs from the GV clearance gap and has significant impact on turbine performance.

Increasing number of hydropower plants are being built in the regions where rivers are heavily loaded with sediments. High concentration of sediments in flow induces material erosion in turbines. This leads to change in flow pattern, losses in efficiency, vibrations and even final breakdown of components. Due to secondary flows and corner vortex, higher erosion occurs between GV and its wall. Erosion in this region causes further increase of clearance gap. Figure 1 shows typical damages of distributor system of a Francis turbine, operating under heavy sediment load. Deep groves on the mating surfaces gives an indication of level of crossflow occurring from this region. Such high crossflow can completely change the velocity profile at the runner inlet. Change in velocity profile at the inlet causes additional erosion damage and other undesired effects in the turbine runner. It has been reported that more than 25% of runner blade area has been eroded by sediments within 3 years of operation in Nepal's largest power plant [5]. Such scale of erosion in turbine component causes significant loss in hydraulic efficiency and incurs heavy maintenance costs. There has been very limited studies regarding the effects of leakage flow from GV clearance gap on velocity profile at runner inlet of a Francis turbine.

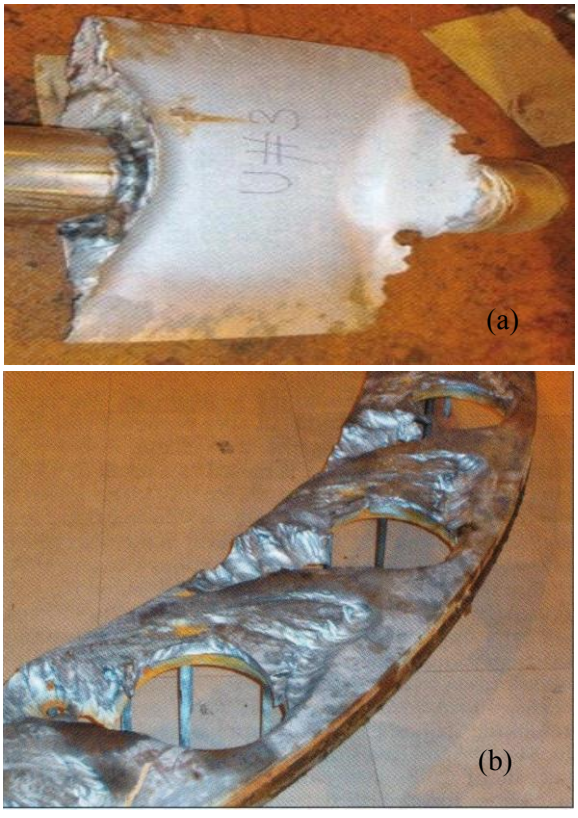

Figure 1. Sediment erosion damage: (a) in GV, (b) in facing plates [4]

A test setup is developed, at NTNU, for the experimental investigations of flow around guide vanes of Francis turbines [6]. The test setup is able to produce steady flow conditions from the position of stay vane outlet to the runner inlet of a low specific speed Francis turbine. The design goal is to acquire similar flow conditions as that observed in a prototype Francis turbine. The objective of this setup is to examine the effects of leakage flow around guide vanes on flow conditions at runner inlet. The setup isolates effects of runner on the flow field and hence allows study of effects of leakage flow alone on the flow conditions at the position of runner inlet. This paper briefly discusses design procedure followed to develop the test setup. The main is to investigate nature of flow from GV clearance gap, and analyze its effects on velocity distribution at the runner inlet.

2. Development of Test Setup

2.1 Reference turbine

Jhimruk Hydroelectric Centre (JHC) in Nepal is considered as the reference case for this study. The power plant has three units of Francis turbine, each producing 4.2 MW at best efficiency point (BEP). These are splitter bladed Francis turbines as with specific speed 0.086, as defined by equation (1) [7].

$$N_{QE} = \frac{n \cdot Q^{0.5}}{E^{0.75}} \quad \text{(-)} \qquad (1)$$

Where, N_{QE} is specific speed, n is speed of runner (s^{-1}), Q is flow in turbine (m^3/s) and E is specific hydraulic energy of turbine (Jkg^{-1})

This power plant also represents a typical case of projects operating under large sediment load in Himalayan basin [8]. Design and drawings of the prototypes are not available. An in-house tool named as "*Khoj*", was developed to design a reference turbine with the aim to replace with the existing one [9]. Extensive investigations has been carried out on this reference turbine for optimizing hydraulic design to minimize sediment erosion without compromise in efficiency [10-13].

Table 1 presents the relevant analytical values for the reference turbine at BEP. These parameters are used to develop the test setup for this study.

Table 1. Reference turbine analytical design values

S.N.	Parameters	Symbol	Unit	Value
1	Net head	H	m	201.5
2	Flow rate per unit turbine	Q	m^3/s	2.35
3	Rotational speed	N	rpm	1000
4	Specific speed	N_{QE}	-	0.086
5	Number of blades in runner	Z_Blades	-	17
6	Inlet diameter of runner	D_1	m	0.89
7	Number of Guide vanes	Z_gv	-	24
8	Chord length of GV	L_gv	m	0.14

2.2 Design and optimization of flow cascade

A symmetric section of reference turbine forms the flow cascade. Some of the researchers have considered a straight channel with single guide vane [14, 15], while others have considered a section of model turbine to investigate the passage flow conditions [1, 16]. Choice of channel profile depends upon objectives and requirements of the measurements. For the present study, three GV with two flow passages out of 24 passages of the GV is considered as a reference case. This configuration has a single GV inside the flow channel. Two outer GV forms as part of walls of cascade and middle GV guides flow in the channel. Thus this layout of the test setup is named as one GV test setup.

Figure 2 shows the layout of cascade considered as the reference design. Walls defined by the profile of free vortex flow with equation (2) is considered from center of spiral casing to inlet of guide vane, from outlet of guide vane to inlet of runner and from the inlet of runner to outlet of cascade. Stay vanes are not included as part of cascade, as they are mainly for strengthening spiral casing and do not play significant role for hydraulic design [17]. Circular portion of spiral casing is replaced with flat plates with the same height as that of the span of guide vane. Thus, section from inlet to outlet of cascade is embedded between two flat plates. This makes the design relatively simple and easy for manufacturing. However, such simplification would affect the flow conditions and hence the optimization of walls' profile is necessary. CFD based optimization techniques are applied to redesign the profile from the inlet of cascade to the center of spiral casing, and from the inlet of runner to the outlet of cascade until the satisfactory flow conditions are obtained.

$$C_u \cdot R = Constant \qquad (2)$$

(Where Cu is tangential velocity of flow at the radius R from center of turbine)

Profile of wall upstream of the center of spiral casing up to the inlet of cascade is re-designed to develop the necessary flow conditions at the center of spiral casing from completely axial flow at the inlet of cascade. The main criteria to satisfy the optimization goal is to have similar profile of both tangential and radial velocity components, at the position of runner inlet of cascade, as that observed in case of the reference prototype turbine. Details of design optimization and CFD analysis is discussed in earlier work by the same authors [6].

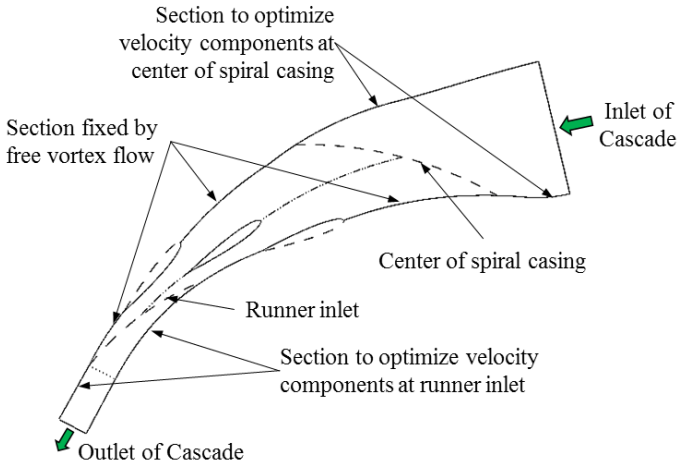

Figure 2. Reference design and sections for optimization

3. Experimental Methods

3.1. Test Setup

Development of the experimental test setup is based on the layout of optimum design of one GV cascade. This configuration re-creates the flow around one GV, inside equivalent two periodic flow channels of a Francis turbine. Angular position covered by the flow passage, inside the cascade, is 30 degrees from the turbine center. This flow passage is 1/12th size of turbine in angular direction. Figure 3 shows the cross section view of the test setup along the plane of measurement. For the convenience of manufacturing, assembly and testing, the setup is divided into parts shown. The test section contains the test guide vane (TGV) inside a plexi-glass flow channel for optical excess to PIV system. Figure 4 shows the cross section view of the test section along GV chord. Position of clearance gap and taps for pressure measurements in the gap can be observed. TGV has been designed as an assembly of multiple parts. Plexi part of TGV imparts transmission of the laser sheet, allowing excess to entire plane inside the flow channel. Other two parts are made of aluminum. The middle part of TGV is attached to the plexi part, and the end part of TGV is screwed with the middle part. The end part of TGV can be replaced with the similar parts of different thickness to get desired clearance gap with respect to the flow channel wall.

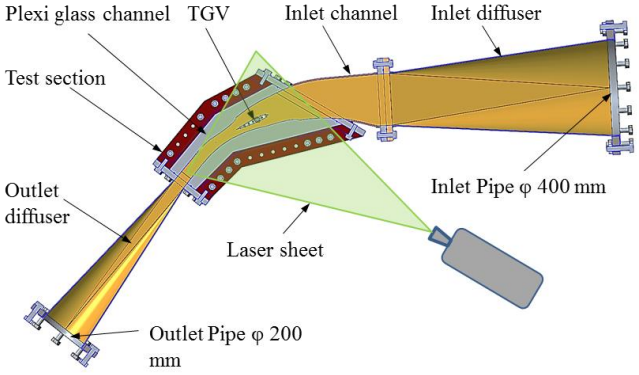

Figure 3. Sectional view of test setup along plane of measurement

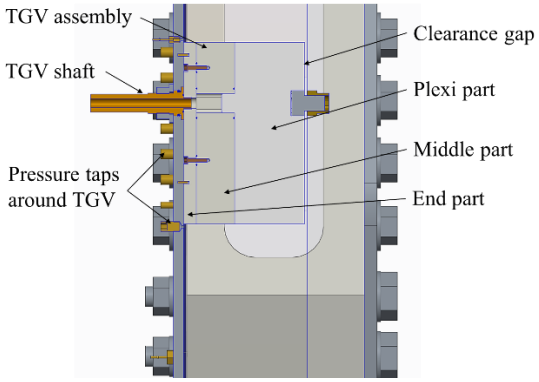

Figure 4. Sectional view of test section along GV chord

The test setup is installed at the facilities of the Waterpower laboratory in NTNU. The setup is mounted in a closed loop system consisting of pump, flow meter, and a pressure tank. Air pressure inside the pressure tank is maintained to atmospheric pressure. All the measurements for this study is conducted with flow rate of 58.2 liter per second. This is 30% of design flow for the same flow area in the prototype at BEP. This is also the maximum flow through the setup for avoiding the cavitation at the

outlet of test section. With this flow, the average velocity obtained at the runner inlet position, is 12.45 m/s. For higher velocities the test setup should be pressurized by applying external pressure in the pressure tank. The external pressure is corresponds to the desired maximum velocity inside test setup while avoiding the cavitation. In order to achieve the prototype flow conditions, maximum pressure inside the test loop could reach up to 10 bars.

3.2. Pressure Measurements

Pressure measurements are done along the TGV surface, close to the test section wall without clearance gap. 14 pressure taps with 2 mm diameter are inserted in the test section cover plate to measure pressure from both pressure and suction side of TGV (Figure 5). These measurements are done at eight different sections along the chord length. Symmetric positions at pressure and suction side of TGV are taken for the measurements at the respective section. Each pressure tap is connected to piezo-resistive pressure transducer through a plastic hosepipe. All the sensors are pre-calibrated against the dead weight calibrator. Measurement uncertainly was maintained to be below 0.05% at all the measuring points. An average of 2000 samples, for each pressure point, measured at 5 HZ, is considered for the pressure analysis.

3.3. Velocity measurements

Particle Image Velocimetry (PIV) method is applied for the velocity measurements. Flow field from the position of stay vane outlet to the position of runner inlet is captured and analyzed. A pulsed light sheet with a thickness of 2 mm, is generated by two double-cavity Nd-YAG lasers providing 120 mJ by pulse. The lighted field is visualized by a HiSense 2M CCD PIV cameras, with a series of paired images acquired at 150 µs and 4 Hz. Alignment of laser and camera with respect to the measurement plane is achieved with separate laser pointers. Fluorescent seeding particles, with a density of 1.016 kg/m^3, refractive index of 1.52 and mean diameter of 55 µm are used during the measurements. The camera resolution is 1280x1024 pixels for a 350x400 mm spatial domain. The PIV system is calibrated using a 2D calibration target. The calibration was performed *'in-situ'* with a specially designed system. The camera exposition, its synchronization with laser and image processing are done with a Dantec DynamicStudio 3.40 PIV specific processor. The image processing is carried out with 32-pixel resolution cross-correlation technique with 50% overlap.

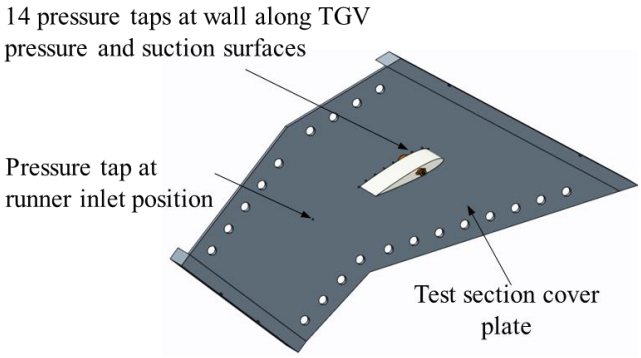

Figure 5. Positions for pressure taps along GV walls

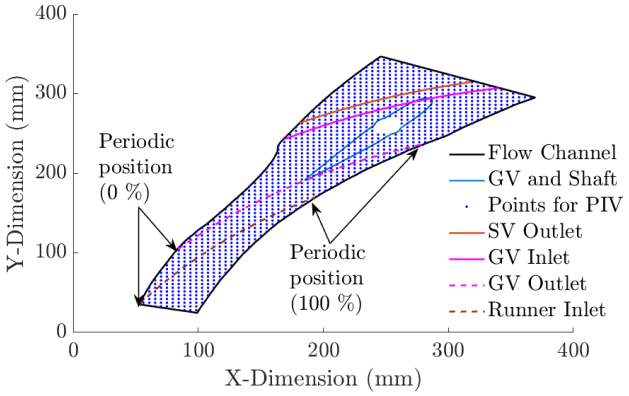

Figure 6. Flow section and positions for velocity study

Figure 6 shows the region of interest from PIV image along the clearance gap. Circumferential position respective turbine components from SV outlet to runner inlet, inside the flow channel, can be observed. Periodic position (PP) between the cascade walls represents 30˚ angular position in circumferential direction with respect to turbine center. It can be observed that the PP from 0% to 50% represents the pressure side of flow, and PP from 50% to 100% represents the suction side of flow respectively. Grid points for each interrogation area for PIV processing can also be seen. Unique velocity vector is obtained for each grid point with the time-averaged value for 100 image pairs. Running

mean convergence test and bad vector position analysis has confirmed that 100 number of image pairs are sufficient to keep the standard deviation of time averaged velocity of good vectors below 0.1% of mean velocity.

Figure 7 shows the measurement planes with respect to position of runner blade in axial view. It can be observed that plane of measurement along GV mid-span corresponds to position of mid-height at runner inlet. Similarly, plane of measurement along clearance gap corresponds to position of hub at runner inlet. For this study measurements are conducted and analyzed at these two planes. Effects of clearance gap on the main flow is studied by comparing the flow conditions at the runner hub with respect to the flow conditions at runner mid-height.

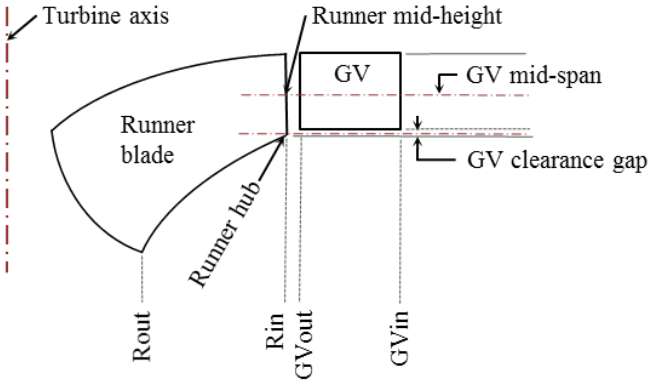

Figure 7. Measurement planes relative to runner blade

4. Results and Discussions

This paper presents the results of pressure and velocity measurements at the flow conditions described in section 3.1. Pressure measurements are done along the pressure and suction side of GV. Velocity measurements are done along plane of GV mid-span and along plane of middle of clearance gap.

Figure 8 shows the pressure distribution along the GV surface. All the pressure values are normalized by the pressure at the leading edge of GV. Highest pressure at the leading edge shows the stagnation point. A clear pattern of pressure and suction side can be observed as the flow progresses towards the trailing edge. Equal distribution of pressure up to 10% of GV chord from the leading edge shows angle of attack close to zero. Gradual development of pressure difference towards trailing edge is observed with maximum pressure difference occurring at 60-70% of the chord length. This pressure difference predicts development of cross flow in case of presence of clearance gap.

Figure 9 shows velocity distribution inside the flow cascade obtained from PIV measurements along the plane of GV mid-span. The basic flow phenomenon as stagnation point at the leading edge of GV, development of flow around pressure and suction sides and formation of wake at the trailing edge can be observed in the velocity contour. Lower velocities along the pressure side of GV and higher for the suction side matches the results from pressure measurements. At the trailing edge, flow from the pressure side has a negative pressure gradient and flow from suction side has a positive pressure gradient (Figure 8). This causes an unbalanced mixing of fluids with different pressure gradients at the trailing

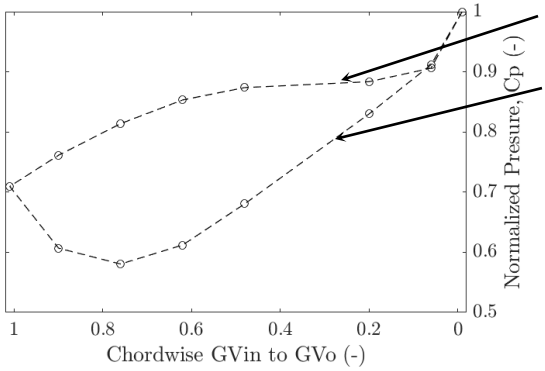

Figure 8. Pressure measurements along GV surface

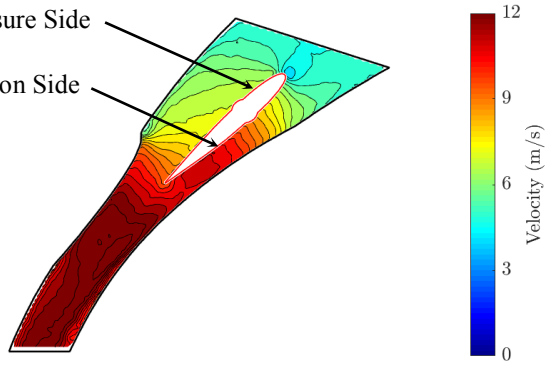

Figure 9. Contour plot of velocity along GV mid-span

edge of GV (Figure 9). Thus velocity and pressure distribution along the circumferential direction of GV outlet in Francis turbine becomes non-uniform. Hence, even in the normal operating conditions, turbine runner passes through different gradients of velocity and pressure as it rotates between two GV. It is also observed, in Figure 9, that the flow around the GV in the middle of flow channel is not identical with the flow around the GV that forms the part of wall in flow channel. It is partly due to the nature of flow without runner and mainly due to single GV in the cascade.

Figure 10 shows the observation of the flow inside test setup for the case of 2 mm clearance gap. As indicated by the pressure measurements, crossflow occurs towards the trailing edge of GV. It can be seen that a vortex filament is developed as the crossflow mixes with the main flow. The filament starts from clearance gap at the 75% of chord length, from the suction side, and is carried downstream towards the position of runner inlet. As the flow moves downstream of GV, location of the filament appears to be shifted towards the suction side due to pressure gradients. The filament diffuses with main flow as it approaches outlet of test section, where flow becomes more uniform.

Figure 11 shows the results of PIV measurements at the plane middle of 2 mm clearance gap. Contours of total velocity together with the velocity vectors can be observed. Close to the leading edge velocity vectors are close to that of main stream flow both in magnitude and direction. Stagnation of flow by the GV shaft can also be seen. Behind the GV shaft gradual development of crossflow and its mixing with main stream flow can be observed. As also indicated by the pressure measurements, the highest amount of crossflow, both in magnitude and direction, occurs at 60-70% of chord length. Mixing of cross flow with main flow seen in Figure 11 justifies the formation and development of vortex filament as observed in Figure 10.

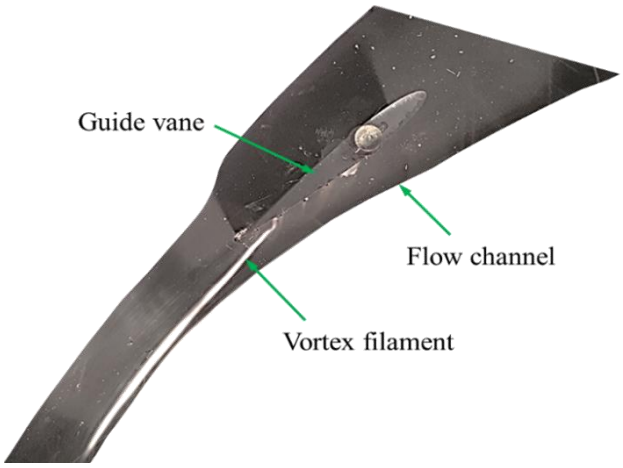

Figure 10. Observation of vortex filament from clearance gap

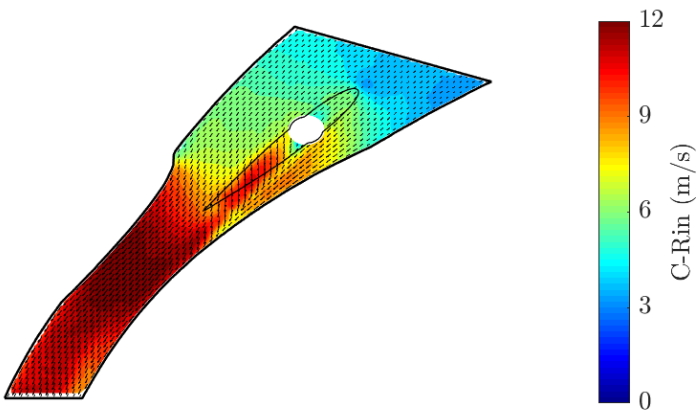

Figure 11. PIV measurements of flow felid along clearance gap

A term 'Velocity Ratio (VR)' is defined, as equation (3).VR measure the change in respective velocity components along any GV span with respect to velocity components along GV-mid span. Thus, along the GV mid-span VR is 1 for all velocity components, at all locations and all periodic positions. Change in VR for other GV spans, at each location, e.g. runner inlet, indicates disturbance of clearance flow on respective velocity components at that location.

$$\boldsymbol{Velocity\ Ratio\ (VR)} = \frac{\boldsymbol{Velocity\ component\ along\ any\ GV\ span}}{\boldsymbol{Velocity\ component\ along\ GV\ mid-span\ at\ the\ same\ location}} \quad \textbf{(-)} \qquad (3)$$

Figure 12 shows VR at the runner inlet position along the plane of clearance gap. Thus this figure demonstrates the relative distortion of each velocity components at the runner inlet due clearance gap. Velocity components along the circumferential direction is presented. It can be seen that at the clearance gap, the radial component of velocity has increased by more than 3.5 times than that at the mid-span. The other two velocity components have reduced proportionality. Since magnitude of radial component is very small with respect to the tangential component, vector law of velocity components is still valid with such seemingly unproportioned change in VR for individual velocity components. Deviations in velocity components occurring towards the suction side (50-100% PP), matches with the location of crossflow and vortex filament being at the same location (Figure 11). This indicates that velocity components, at the runner inlet, are non-uniform, in both angular direction and span wise direction, due to disturbance of crossflow originating from the clearance gap.

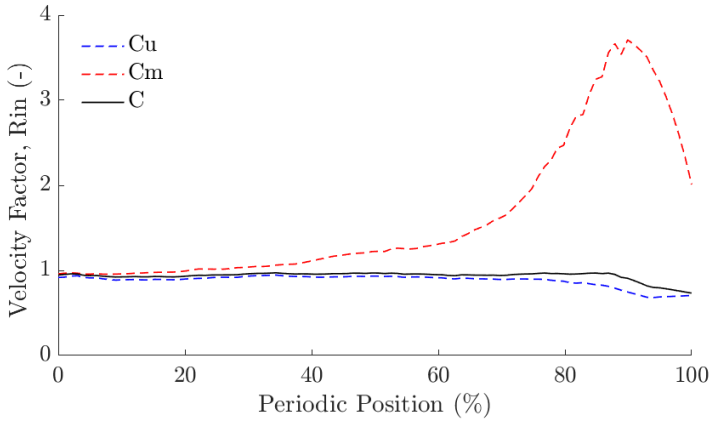

Figure 12. Velocity components at runner inlet along clearance gap

Figure 13 shows effects of clearance flow on the velocity conditions at the runner inlet. Based on PIV results, proportionate velocity triangles are drawn at position of mid-height and hub at runner inlet (Figure 7). It is seen that the distorted velocity component at runner hub has significant effects on inlet flow conditions. Close to hub tangential velocity is reduced by 26% and radial velocity is increased more than 3.5 times. This causes relative velocity at the hub to be increased by 3.8 times than that at the middle of inlet height. Such changes on tangential and relative velocity at runner inlet have considerable consequences on turbine performance.

Euler turbine equation defines the turbine efficiency in terms of tangential velocities at runner inlet and outlet respectively as equation (4):

$$\boldsymbol{\eta_h} = \frac{\boldsymbol{Cu1 \cdot U1 - Cu2 \cdot U2}}{\boldsymbol{gH}} \quad \textbf{(-)} \qquad (4)$$

Where η_h is hydraulic efficiency of turbine, *Cu* is the tangential velocity, *U* is runner peripheral velocity, *g* is acceleration due to gravity and *H* is pressure head at runner. *1* & *2* are subscripts for inlet and outlet respectively. Equation (4) shows that reduction of tangential velocity towards hub due to clearance flow causes on direct loss in turbine efficiency. However, this analysis does not include the runner, which will have an effect on the velocity distribution.

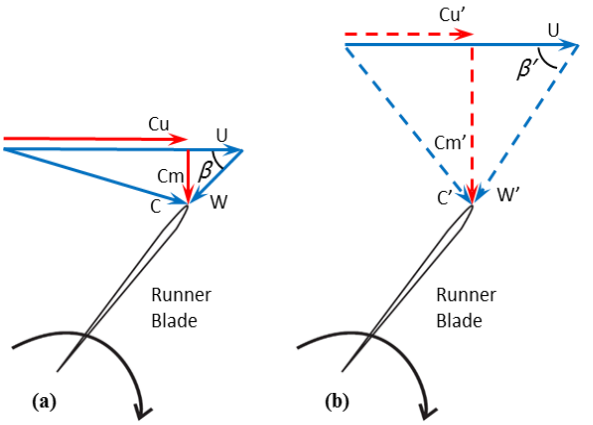

Parameter	Symbol	Unit	Mid	Hub	VR
Tangential velocity	Cu	m/s	11.68	8.69	0.74
Radial velocity	Cm	m/s	1.67	6.21	3.72
Total velocity	C	m/s	11.78	10.69	0.91
Relative velocity	W	m/s	1.93	7.35	3.81
Runner inlet angle	β	deg	60.01	57.68	0.96
Runner peripheral velocity	U	m/s	12.63	12.63	1

Figure 13. Velocity conditions at runner inlet: (a) at mid-height, (b) at hub with 2 mm clearance gap

Studies have shown that sediment erosion on turbine components is proportional to third power of relative velocity [18]. Thus such a high increase in relative velocity at around hub of runner at the inlet would causes severe erosion this location. Furthermore, non-uniform relative velocity long runner height and also between adjacent blades would cause secondary flows and turbulence. These effects may further accelerate erosion of blade surfaces and cause further loss in efficiency.

Several cases of severe erosion at the runner hub have also been reported by past authors [4, 19]. Figure 14 shows a typical case of sediment erosion at runner hub, together with erosion in GV walls at trailing edge [19]. Significant loss in turbine efficiency, due to erosion, has also been reported. On basis of the presented results, these phenomenon can be explained as follows. Symmetric NACA profile has been used to shape the GV geometry. Thus, higher pressure difference towards trailing edge of GV causes higher secondary flows and corner vortex. This causes higher erosion at walls of the GV trailing edge. Erosion in GV trailing edge induces strong crossflow, which reduces tangential velocity and increases relative velocity at runner hub. Losses in turbine efficiency can be correlated with reduction in tangential component and the erosion at runner hub can be correlated with increase in relative velocity.

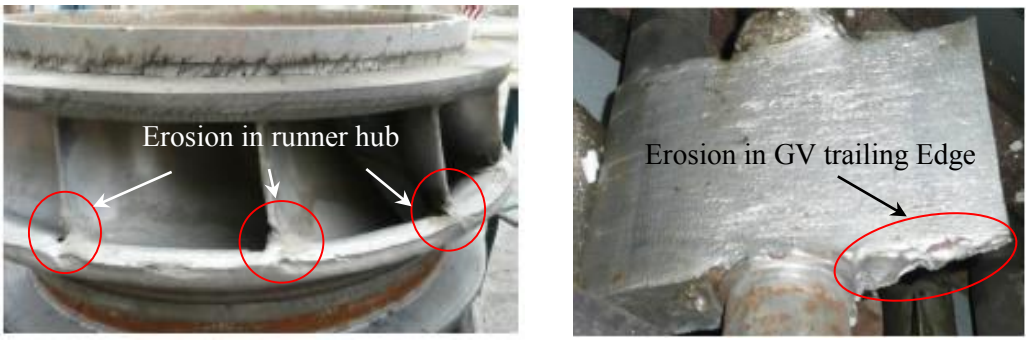

Figure 14. Erosion of Francis Turbine components: (a) Runner hub, (b) Guide vane [19]

5. Conclusions:

A test setup has been developed to investigate flow conditions around guide vane of low specific speed Francis turbine. The setup includes flow passage with one guide (GV), which is able to create similar velocity conditions as in a prototype turbine. NACA 0012 airfoil has been taken as a reference profile to shape GV. Presented measurements are conducted at 30% flow of prototype at BEP. Pressure and velocity measurements are done to evaluate the effects of GV clearance gap on the flow conditions at runner inlet. It is concluded from this study that a strong crossflow occurs from the GV clearance gap due to high pressure difference between GV surfaces. Relative velocity at runner inlet hub increases more than 3.5 times that that at mid height. This has been related as a cause of high sediment erosion,

often observed around inlet hub of Francis runner, operating in sediment laden projects. Crossflow also causes lowering of runner efficiency by reduction in tangential velocity at close to hub. Further investigation on characteristics of vortex filament developed by the crossflow is necessary, to identify its effects on turbine performance and life. Study of alterative profiles for GV can help to identify better designs of GV for sediment laden projects. A cascade with three GV inside flow channel would be developed for further investigation of problem under consideration.

References:

[1] X. Chen, "Theoretical and experimental study of flow through the double cascade of a Francis turbine," PhD thesis, Norwegian University of Science and Technology, Faculty of Engineering Science and Technology, 1992.
[2] S. Eide, "Numerical analysis of the head covers deflection and the leakage flow in the guide vanes of high head Francis turbines," 2004.
[3] H. Brekke, "The influence from the guide vane clearance gap on efficiency and scale effect for Francis turbines," in *Proc. 14th IAHR Symposium on Progress within Large and High-Specific Energy Units*, 1988, pp. 825-837.
[4] H. K. Sharma, "Power generation in sediment laden rivers: The case of Nathpa Jhakri," *International Journal on Hydropower and Dams*, vol. 17, pp. 112-116, 2010.
[5] B. Chhettry, B. Thapa, and B. S. Thapa, "Assembly design to ease turbine maintenance in sediment-laden conditions," *International journal on hydropower and dams*, pp. 82-88, 2014.
[6] B. S. Thapa, C. Trivedi, and O. G. Dahlhaug, "Design and development of guide vane cascade for a low specific speed Francis turbine," *Journal of Hydrodynamics, Ser. B,*, Accepted on 22 November, 2015.
[7] IEC, "Hydraulic turbines, storage pumps and pump-turbines – Model acceptance tests 2nd edn 1999-11," in *IEC 60193*, ed: The International Electro technical Commission, 1999.
[8] P. M. S. Pradhan, O. G. Dahlhaug, P. N. Joshi, and H. Støle, "Sediment and Efficiency Measurements at Jhimruk Hydropower Plant – Monsoon 2003," Report from HydroLab, Nepal2004.
[9] B. S. Thapa, "Hydraulic design of Francis turbine to minimize sediment erosion," Masters Thesis, Kathmandu University, 2012.
[10] B. S. Thapa, M. Eltvik, K. Gjøsæter, O. G. Dahlhaug, and B. Thapa, "Design Optimization of Francis Runners for Sediment Handling," in *Fourth International Conference on Water Resources and Renewable Energy Development in Asia, Thailand*, 2012.
[11] B. S. Thapa, B. Thapa, M. Eltvik, K. Gjosater, and O. G. Dahlhaug, "Optimizing runner blade profile of Francis turbine to minimize sediment erosion," in *IOP Conference Series: Earth and Environmental Science*, 2012, p. 032052.
[12] S. Chitrakar, M. Cervantes, and B. S. Thapa, "Fully coupled FSI analysis of Francis turbines exposed to sediment erosion," *International Journal of Fluid Machinery and Systems*, vol. 7, pp. 101-109, 2014.
[13] B. Rajkarnikar, H. P. Neopane, and B. S. Thapa, "Development of rotating disc apparatus for test of sediment-induced erosion in francis runner blades," *Wear*, vol. 306, pp. 119-125, 2013.
[14] F. Bario and C. Beral, "Boundary layer measurements on the pressure and suction sides of a turbine inlet guide vane," *Experimental Thermal and Fluid Science*, vol. 17, pp. 1-9, 1998.
[15] A. Zobeiri, P. Ausoni, F. Avellan, and M. Farhat, "How oblique trailing edge of a hydrofoil reduces the vortex-induced vibration," *Journal of Fluids and Structures*, vol. 32, pp. 78-89, 2012.
[16] Z. Schabowski and H. Hodson, "The Reduction of over tip leakage loss in unshrouded axial turbines using winglets and squealers," *Journal of Turbomachinery*, vol. 136, 2014.
[17] Z. Wei, P. H. Finstad, G. Olimstad, E. Walseth, and M. Eltvik, "High Pressure Hydraulic Machinery," in *Compendium*, N. Publication, Ed., ed, 2009.
[18] B. S. Thapa, O. G. Dahlhaug, and B. Thapa, "Sediment erosion in hydro turbines and its effect on the flow around guide vanes of Francis turbine," *Renewable and Sustainable Energy Reviews*, vol. 49, pp. 1100-1113, 2015.
[19] O. G. Dahlhaug, P. E. Skåre, V. Mossing, and A. Gutierrez, "Erosion resistant coatings for Francis runners and guidevanes," *International Journal on Hydropower and Dams*, vol. 17, pp. 109-112, 2010.